iScience

CellPress

Article

# Human Antibody Repertoire following Ebola Virus Infection and Vaccination

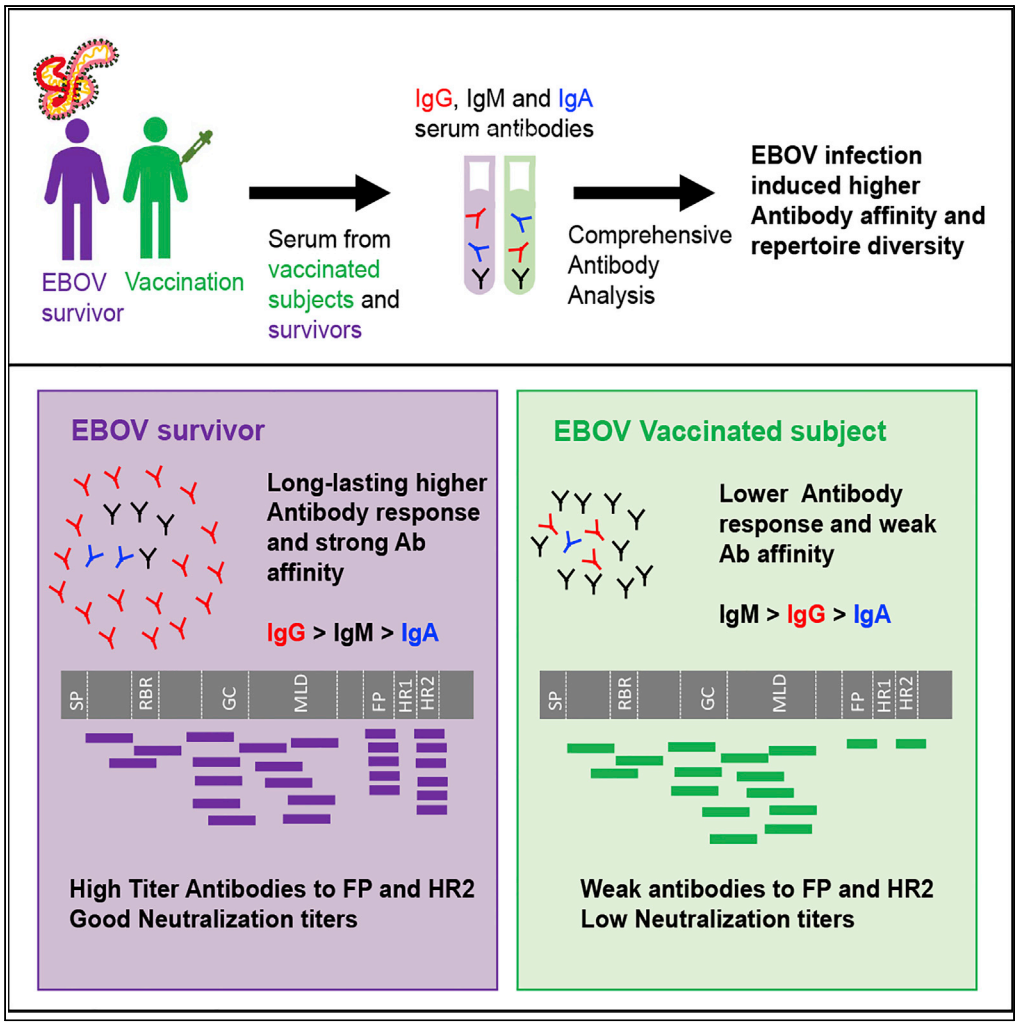


Sandra Fuentes, Supriya Ravichandran, Elizabeth M. Coyle, Laura Klenow, Surender Khurana

surender.khurana@fda.hhs.gov

## HIGHLIGHTS

EBOV infection induced a more diverse antibody repertoire than vaccination

Ebola survivors demonstrated long-lasting, high-affinity, IgG antibody response

Several novel antigenic sites recognized by post-EBOV infection sera

Fuentes et al., iScience *23*, 100920
March 27, 2020
https://doi.org/10.1016/j.isci.2020.100920

iScience

CellPress

Article

# Human Antibody Repertoire following Ebola Virus Infection and Vaccination

Sandra Fuentes,[1] Supriya Ravichandran,[1] Elizabeth M. Coyle,[1] Laura Klenow,[1] and Surender Khurana[1,2,*]

## SUMMARY

**Limited knowledge exists on the quality of polyclonal antibody response generated following Ebola virus (EBOV) infection compared with vaccination. Polyclonal antibody repertoire in plasma following EBOV infection in survivors was compared with ChAd3-MVA prime-boost human vaccination. Higher antibody binding and affinity to GP was observed in survivors compared with vaccinated plasma that correlated with EBOV neutralization. Surprisingly, a predominant IgM response was generated after prime-boost vaccination, whereas survivors demonstrated IgG-dominant antibody response. EBOV infection induced more diverse antibody epitope repertoire compared with vaccination. A strong binding to antigenic sites in the fusion peptide and another in the highly conserved GP2-HR2 domain was preferentially recognized by EBOV survivors than vaccinated individuals that correlated strongly with EBOV neutralization titers. These findings will help development and evaluation of effective Ebola countermeasures including therapeutics and vaccines.**

## INTRODUCTION

Ebola virus causes severe and often fatal disease in humans and is considered a global public health priority. The ongoing outbreak of highly pathogenic Zaire Ebola virus (EBOV) in Democratic Republic of the Congo (DRC) has resulted in more than 3,393 human cases and 2,235 deaths (case fatality rate = c. 67%) as of 9 January, 2020 (https://www.who.int/emergencies/diseases/ebola/drc-2019). This follows the devastating 2014 EBOV epidemic in Western Africa that resulted in more than 28,652 human cases and 11,325 deaths and outbreaks in DRC in 2014 and 2017. Moreover, since the virus might persist in some survivors (Mate et al., 2015), it is feared that EBOV epidemics could continue to recur, resulting in severe epidemics. Therefore, development of an effective vaccine against Ebola is a high priority (Kanapathipillai et al., 2014). Multiple vaccine candidates are being evaluated in humans in clinical trials, with the rVSV-EBOV vaccine now being licensed in the United States and Europe (Ewer et al., 2016; Henao-Restrepo et al., 2015; Jones et al., 2005; Kennedy et al., 2017; Krause, 2015; Marzi et al., 2015a, 2015b; Milligan et al., 2016; Rampling et al., 2016; Regules et al., 2017; Tapia et al., 2016). Both T cell and B cell immunity plays an important role in providing protection against Ebola virus disease (EVD) (Ruibal et al., 2016). Since passive transfer of antibodies in animal models have shown to protect the NHPs against lethal EBOV challenge, several antibody-based therapeutics are also in clinical trials (Dye et al., 2012; Holtsberg et al., 2015; Marzi et al., 2013). It is postulated that immune responses generated following EBOV infection in survivors may provide life-long protection against EBOV (Crook et al., 2017). Primarily ELISA and EBOV-neutralization tests have been used to analyze the anti-EBOV antibodies, but these assays provide limited insight into the diversity and quality of polyclonal antibody response generated following EBOV infection and how they compared with those generated following vaccination in humans (Blaney et al., 2013; Matassov et al., 2015; Wong et al., 2012). Previously, we described the antigenic fingerprint generated following homologous prime-boost vaccination with a recombinant vesicular stomatitis virus (rVSV)-based vaccine expressing the EBOV surface glycoprotein (GP) from the Kikwit 1995 strain (rVSVΔG-ZEBOV-GP). The effectiveness of this vaccine was demonstrated in a ring vaccination study in Guinea during an outbreak in 2015 (Henao-Restrepo et al., 2015; Khurana et al., 2016). This rVSVΔG-ZEBOV-GP vaccine is being used extensively in the ongoing outbreak in DRC and was recently approved by the US Food and Drug Administration (FDA) for prevention of disease caused by Zaire ebolavirus in individuals 18 years and older.

In this study, we performed comprehensive analysis of the humoral immune response following EBOV infection in survivors and following prime-boost vaccination with live ChAd3-MVA prime-boost vaccine in healthy adult volunteers (Ewer et al., 2016; Wilkinson et al., 2017). ChAd3-MVA is a monovalent formulation of the chimpanzee adenovirus 3 (ChAd3)-vectored vaccine encoding the surface glycoprotein of EBOV/Mayinga and boosted with the same ebolavirus gene in a modified vaccinia Ankara (MVA)-vectored

[1]Division of Viral Products, Center for Biologics Evaluation and Research (CBER), Food and Drug Administration (FDA), 10903 New Hampshire Avenue, Silver Spring, MD 20993, USA

[2]Lead Contact

*Correspondence: surender.khurana@fda.hhs.gov

https://doi.org/10.1016/j.isci.2020.100920

vaccine that also contains genes encoding Sudan ebolavirus and Marburgvirus glycoprotein and Tai Forest nucleoprotein. Quantitative and qualitative analyses of polyclonal plasma were performed to elucidate antibody epitope repertoires using gene fragment-phage display libraries (GFPDL) and surface plasmon resonance (SPR) technology to measure real-time antibody binding kinetics, antibody cross-reactivity, immunoglobulin isotypes, affinity, and antibody specificity to each of the antigenic sites identified using GFPDL. Technically, since antibodies are bivalent, the proper term for their binding to multivalent antigens like viruses is avidity, but here we use the term affinity throughout since we do not describe any monovalent interactions. The focus was to identify the overall global pattern of antibody epitope diversity generated following human EBOV infection versus vaccination rather than fine antibody specificities in each individual. Previously, GFPDL spanning the entire genome of highly pathogenic avian influenza virus, human immunodeficiency virus, and Respiratory syncytial virus was used to map the antibody repertoires of convalescent sera from infected individuals and pandemic influenza vaccinations, which revealed several diagnostic and protective targets (Fuentes et al., 2016; Khurana et al., 2006, 2009, 2010, 2011a, 2011b; Lee et al., 2018).

## RESULTS

### Real-Time Antibody Binding Kinetics of Post-EBOV Infection Plasma and Vaccination Plasma to EBOV GP

A high-titer and a low-titer pool (samples #58 and #64, respectively) of human plasma from individuals primed with ChAd3-vectored EBOV/Mayinga GP and boosted with MVA-vectored EBOV/Mayinga GP, SUDV GP, MARV GP, and TAFV nucleoprotein were obtained as a part of a WHO collaborative study (originally from Oxford, UK vaccine trial). Individual plasma from three survivors from the 2014 Western Africa EBOV outbreak were obtained at 2 (sample #43), 3 (sample #79), or 6 (sample #28) months post-EBOV infection (pi), and a pooled convalescent plasma (sample #92) was obtained from six Sierra Leone patients who recovered from EVD and did not receive any experimental treatment (Table S1). Since no individual vaccinated serum was tested in this study, all antibody comparisons between vaccination versus EBOV infection reflects individual/pooled EVD survivor samples with pooled ChAd3-MVA vaccinee samples. The samples were tested for neutralizing antibodies against a wild-type EBOV strain in a BSL4 laboratory and against a VSV virus expressing the EBOV GP in a pseudovirus neutralization (PsVN) assay (Wilkinson et al., 2017).

We performed quantitative and qualitative SPR analyses for several dilutions of post-vaccination and post-infection polyclonal plasma using a recombinant full-length GP corresponding to the Makona EBOV strain produced in a mammalian system, representing mature GP1 and GP2 domains observed in virions or infected cells (see Transparent Methods). The protein density on the chip was optimized such as to measure only monovalent interactions so that they are independent of the antibody isotype (Khurana et al., 2019). Raw sensorgram for a representative survivor plasma (#58) dilutions is shown in Figure S1. Antibody binding titers of different dilutions of individual samples were measured in resonance units (RU) by SPR (Figure 1). GP-binding antibodies were not detected in negative control plasma (#36). Post ChAd3-MVA vaccination plasma showed lower binding to GP (mean RU = 17 for #64 and 104 for #58 at 10-fold dilution) relative to all four EBOV survivor plasma samples (mean RU = 437 for #43, 2 months pi, 684 for #79, 3 months pi, and 1,040 for #92 at 10-fold dilution, respectively). The RU of the fourth EBOV survivor plasma sample (#28, at 6 months pi) was 14-fold greater than that of ChAd3-MVA plasma sample #64 (219 versus 17), whereas the difference in RU was 2-fold between sample #28 and ChAd3-MVA plasma sample #58 (219 versus 104). Similar antibody binding patterns were observed for these plasma samples to complete EBOV-GP bearing pseudovirion particles. A statistically significant correlation was observed between the *in vitro* EBOV neutralization titers and the plasma anti-GP-binding antibody titers as measured by SPR following vaccination or infection ($r = 0.911$; $p = 0.0008$) (Figure 1B).

To further evaluate anti-GP antibody affinity following vaccination and EBOV infection, the antibody-antigen complex dissociation rates (off-rate constants) were determined as a surrogate for antibody affinity using SPR. Antibody dissociation kinetics of antigen-antibody complexes are independent of antibody concentration and provide a measure of overall average affinity of polyclonal antibody binding (Khurana et al., 2011b, 2016). To that end, serially diluted plasma at 10-, 100-, 200-, 400-, and 800-fold dilutions were injected at a flow rate of 50 μL/min (120-s contact time) for association, and dissociation was performed over a 600-s interval (at a flow rate of 50 μL/min) (Figure S1). Antibody off-rate constants, which describe the fraction of antigen-antibody complexes that decay per second, were determined directly from the plasma antibody interaction with GP in the dissociation phase only for the sensorgrams with

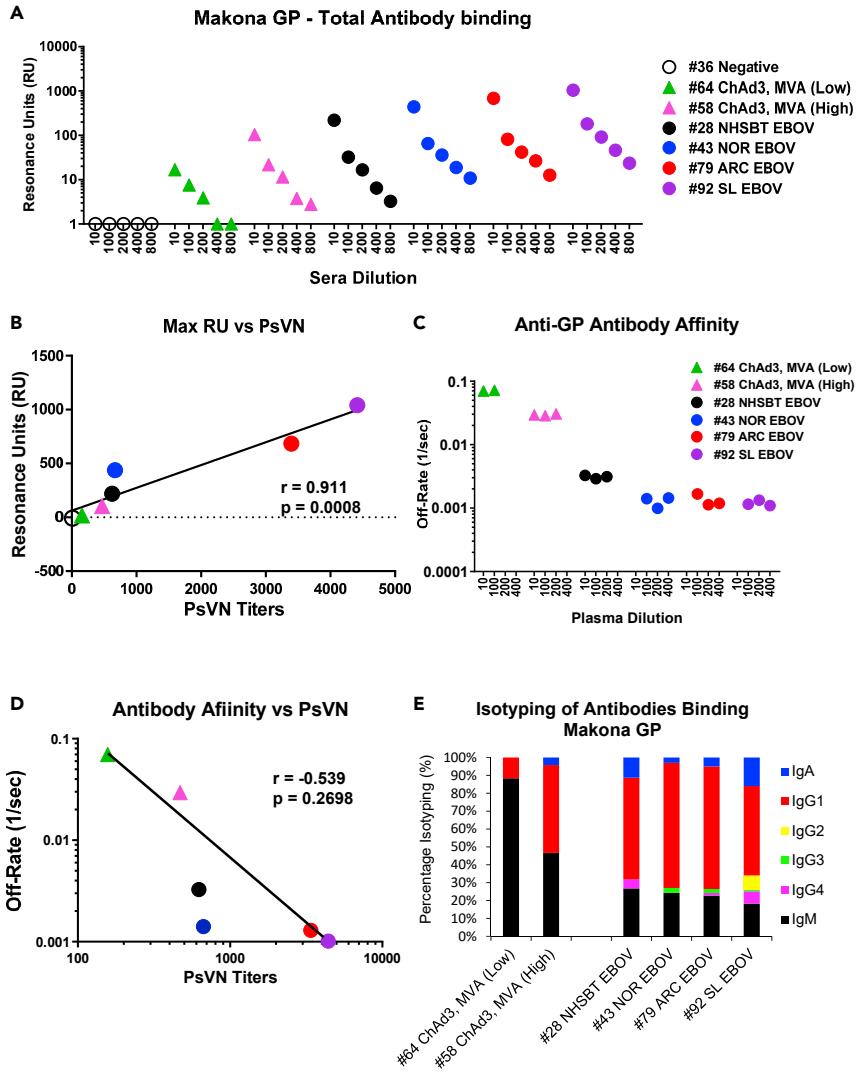


**Figure 1. SPR-Based Analysis of Human Plasma from EBOV-Infected Survivors and following ChAd3-MVA Vaccination to EBOV-GP Purified Protein**

(A) Serial dilutions of plasma samples collected from EBOV survivors (#28, black; #43, blue; #79, red; and #92, purple) or humans vaccinated with ChAd3-MVA vaccine (#58, pink triangle and #64, green triangle) or control (#36, empty circle) were analyzed for total binding to purified mature GP from EBOV/Makona strain by SPR. Total antibody binding is represented in SPR resonance units.

(B) Total GP-binding antibody (Max RU) of human plasma against EBOV/Makona GP correlated with the homologous virus neutralization titers (PsVN; $r = 0.911$, $p < 0.0008$). Pearson correlations are reported for the calculation of correlations between total anti-GP antibody binding and PsVN titers.

(C) Polyclonal antibody affinity to EBOV GP following ChAd3-MVA vaccination or EBOV infection in survivors. Binding affinity of serially diluted post-vaccination and post-infection plasma to EBOV/Makona-GP. Antibody off-rate constants that describe the fraction of antibody-antigen complexes decaying per second were determined directly from the plasma sample interaction with EBOV/Makona-GP using SPR in the dissociation phase as described in Methods.

(D) Correlation between anti-GP-binding antibody affinity as measured by antibody dissociation rates (off-rates) and homologous virus neutralization titers (PsVNA80; $r = -0.539$, $p = 0.2698$). The color scheme in (B)–(D) is the same as that in (A).

(E) Antibody isotype of GP-binding antibodies following EBOV infection or ChAd3-MVA vaccination. The isotype composition of plasma antibodies bound to GP of EBOV/Makona isolate as measured in SPR. The resonance units for each anti-GP antibody isotype was divided by the total resonance units for all antibody isotypes combined to calculate the percentage of each antibody isotype for individual plasma.

maximum RU in range of 10–100 RU using SPR (Figure S1). The off-rates of polyclonal plasma antibodies bound to GP were much slower (indicating stronger antibody affinity) in EBOV survivors (0.00327/s for #28, 0.001407/s for #43, 0.00129/s for #79, and 0.00101/s for #92) in comparison with ChAd3-MVA vaccine recipients (0.0699/s for #64 and 0.0294/s for #58), even though the total anti-GP-binding antibodies of post-vaccination plasma #58 were comparable with those of post-infection sample #28 (Figures 1C and 1A). A correlation was observed between the plasma anti-GP-binding antibody affinity with *in vitro* EBOV neutralization titers that did not reach statistical significance ($r = -0.539$; $p = 0.2698$) (Figure 1D). These observations suggest that the EBOV infection promoted 10- to 60-fold higher antibody affinity (based on antigen-antibody dissociation rates) to GP compared with antibodies induced by ChAd3-MVA prime-boost vaccination.

### Majority of the GP-Binding Antibodies after EBOV Infection Are IgG Isotype, whereas Post-Vaccination-Induced Antibodies Contain Large IgM Component

Isotype analysis of GP-binding antibodies was performed by SPR that demonstrated representation of all isotypes (IgA, IgG, IgM) and IgG subclasses in the post-infection/vaccination plasma (Figure 1E). Secondary MAb analytes with similar affinity/binding patterns with specificity against Fc region of human IgG1, IgG2, IgG3, IgG4, IgA, or IgM were used for isotyping. The anti-GP-binding antibodies in survivor plasma comprised 60%–70% IgG isotype predominated by the IgG1 subclass. Three of four survivor plasma contained 0.7%–2.7% of IgG3 and 1.5%–6.9% of IgG4 GP-bound antibody isotype. Plasma sample #92 obtained from six EVD survivors in Sierra Leone (who did not receive any experimental treatment) contained 8.3% GP-binding antibodies of IgG2 isotype. In contrast, only 12% (#64) or 49% (#58) of the GP-binding antibodies were of IgG isotype even after prime-boost ChAd3-MVA vaccination, with 88% (#64) or 46% (#58) of GP-binding antibodies representing IgM isotype antibodies (Figure 1E), similar to the observation of high IgM response following rVSV-ZEBOV-GP prime-boost vaccination (Khurana et al., 2016). No GP antibody binding for negative control plasma (#36) excluded the possibility that this IgM response following vaccination or infection may be due to polyreactive natural antibodies (i.e., sticky antibodies not induced by GP). Furthermore, in our previous study, the purified IgM antibodies following the rVSV-ZEBOV-GP vaccination showed EBOV neutralizing activity confirming the GP specificity of IgM binding antibodies in SPR (Khurana et al., 2016). GP-bound IgA antibodies ranged from 3% to 15% in EBOV survivors plasma compared with 4.2% in ChAd3-MVA post-vaccination plasma (#58).

### Antigenic Fingerprint of Antibodies Generated following ChAd3-MVA Vaccination Compared with Antibodies from Ebola Virus Disease Survivors

To analyze the epitope repertoire recognized by polyclonal antibodies in plasma from ChAd-MVA-vaccinated and EBOV-exposed subjects, GFPDL containing fragments of the *GP* gene from EBOV/Makona (Figure S2), ranging from 50–1,000 bp in length were generated with $>10^{7.1}$ unique phage clones (see Transparent Methods). The EBOV-GP-GFPDL displayed both linear and conformational epitopes with random distribution of size and sequence of inserts that spanned the entire GP (Figure S3). The GP sequence of EBOV/Makona differs from that of EBOV/Mayinga, used in the vaccine, by 20 amino acids (Figure S4). We have previously shown that this GFPDL represents both linear and conformational epitopes, as determined by mapping a panel of conformation-dependent EBOV neutralizing/protective MAbs. Furthermore, the EBOV-GFPDL adsorbed most EBOV-GP-specific antibodies in the post-vaccination polyclonal human sera (Fuentes et al., 2018; Khurana et al., 2016). To further confirm, in this study ~90% of antibodies from high-titer post-infection survivor plasma sample #79 binding specific to GP were removed by adsorption with the EBOV-GP GFPDL (Figure S5). Together, the epitope mapping of MAbs and adsorption studies using post-vaccination polyclonal sera previously (Fuentes et al., 2018; Khurana et al., 2016) and post-infection plasma herein provided support for using the EBOV-GP GFPDL to dissect the polyclonal antibody repertoires in human plasma.

To compare the polyclonal antibody epitope repertoire generated following ChAd3-MVA prime-boost vaccination with that generated following EBOV infection in survivors, individual plasma specimens from survivors (#28, #43, and #79), pooled EVD Sierra Leone survivor plasma (#92), and pooled plasma from vaccinated individuals with either high (#58) or low (#64) EBOV neutralization titer were used for EBOV-GFPDL analysis (Table S1, Figure 2). The idea was to identify the overall average global pattern of antigenic fingerprint generated following EBOV infection versus vaccination rather than fine specificities of antibodies in each individual. Previous study with rVSV-EBOV GP vaccination in humans showed that the antibody epitope profile in pooled post-vaccination sera was overall similar to the epitope fingerprint determined for individual post-vaccination sera (Khurana et al., 2016).

A

| | POST-EBOV INFECTION | | | | POST-VACCINATION | |
|---|---|---|---|---|---|---|
| | #28 | #43 | #79 | #92 | #58 | #64 |
| Phage Titer | $9.5x10^5$ | $1.5x10^6$ | $8.5x10^6$ | $4.53x10^6$ | $5.4x10^6$ | $1.3x10^6$ |

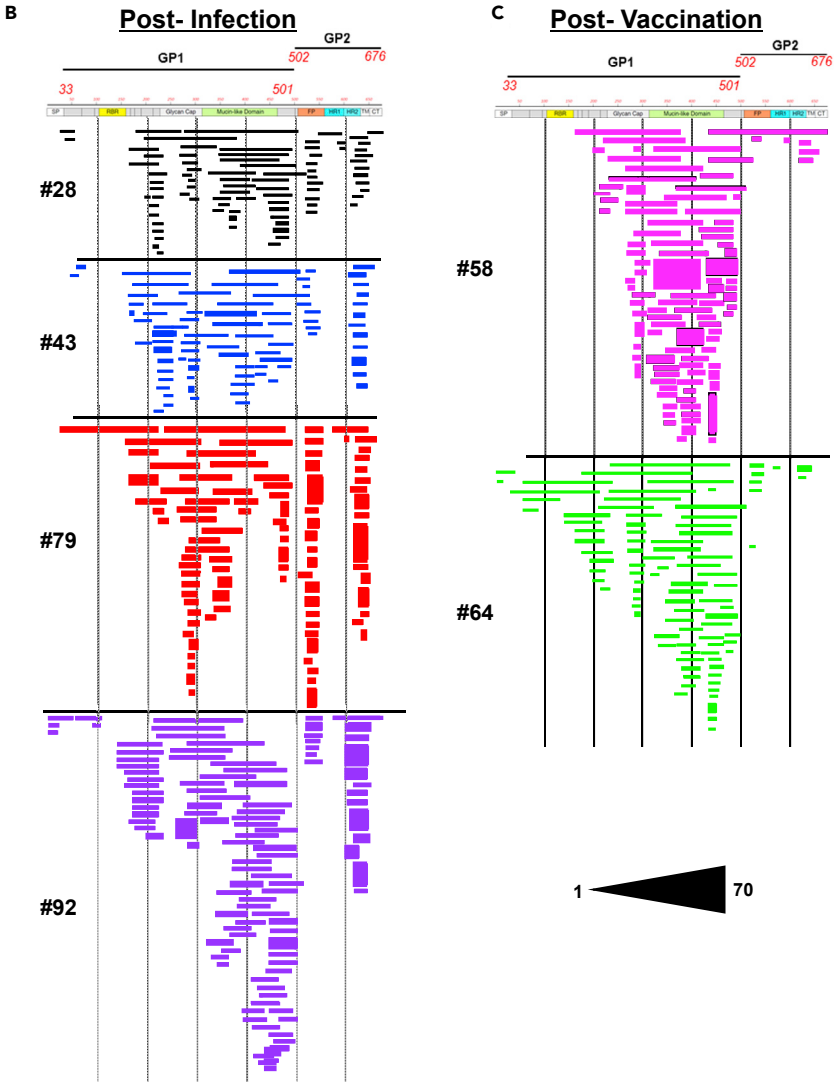


**Figure 2. Antibody Repertoires Elicited following ChAd3-MVA Vaccination or EBOV Infection in Survivors**

(A) Number of captured phage clones isolated using EBOV-GFPDL affinity selection with plasma obtained from EBOV-infected survivors or following ChAd3-MVA vaccination.

(B and C) Schematic alignment of the peptides recognized by the three EBOV-infected survivors' plasma (B) or high-neutralization-titer (#58) and low-neutralization-titter (#64) plasma (C) from ChAd3-MVA vaccinated adults, identified by panning with EBOV-GFPDL. The amino acid designation is based on the GP protein sequence encoded by the complete *EBOV-GP* gene of EBOV/Makona (Figure S2). The GP receptor-binding region (RBR) is depicted as yellow, MLD is shown in light green, the fusion peptide is shown in orange, and the heptad repeats (HR1 and HR2) are shown in cyan. Graphical distribution of representative clones with a frequency of $\geq 2$, obtained after affinity selection, is shown. The horizontal position and the length of the bars indicate the peptide sequence displayed on the selected phage clone to its homologous sequence in the EBOV-GP sequence on alignment. The thickness of each bar represents the frequency of repetitively isolated phage, with the scale shown in the black triangle below the alignment (70 was the highest frequency of a phage clone in this analysis). The dashed lines running vertically refers to the GP amino acid residues 100, 200, 300, 400, 500, and 600.

Negative control human plasma (#36) bound very few phages. For EBOV survivors' plasma, the number of bound phages was highest for sample #79, followed by #92, #43, and then #28 (Figure 2A). For the post-vaccination plasma, sample #58 showed an ~4-fold higher titer compared with the lower-titer (#64) sample ($5.4 \times 10^6$ and $1.3 \times 10^6$ phages, respectively) (Figure 2A). Sequencing of the GP fragments expressed by phages bound by post-infection survivor plasma antibodies showed a diverse epitope repertoire distribution, displaying both small and large sequences (8–247 amino acid residues) spanning across the N-terminal GP1 head domain and to the C-terminal GP2 stalk domain of the Makona GP (Figure 2B). The antibody epitopes mapped to the Glycan cap and mucin-like domain (MLD) and identified immunodominant sites in the fusion peptide at the N terminus of GP2 as well as in heptad repeat (HR)/transmembrane of GP2 for the convalescent samples.

The ChAd3-MVA vaccination generated antibodies focused to epitopes within the glycan cap and MLD of GP1, while lower binding to the fusion peptide and the C terminus of GP2 was observed for post-vaccination samples that were preferentially recognized by post-infection antibodies (Figures 2C versus 2B). In addition, antibodies from the survivors recognized small epitopes in the N-terminal half of Makona GP, and there were more antibodies binding between the RBR and the glycan cap domain compared with the vaccinated plasma pools (Figures 2B and 2C).

## Antigenic Sites within EBOV GP Recognized by Post-Infection and Post-Vaccination Antibodies

Analyses of neutralizing/protective MAbs against EBOV were previously shown to predominantly recognize epitopes within or flanking the MLD, glycan cap, GP1 core, or the base of GP (epitopes for MAb cocktail ZMapp and MAb 114 are depicted in Figure 3A). Survivors of EBOV infection and prime-boost vaccination with ChAd3-MVA generated an antibody response defined by seven antigenic regions (herein referred to as I through VII) with some overlaps (i.e., between regions II and III, III and IV, IV and V, VI and VII) and 21 smaller antigenic sites (II.1 through V.11) within EBOV GP (Figure 3A and Table S2). Several of these antigenic regions/sites were previously identified by post-vaccination antibodies generated following rVSV-EBOV GP vaccination in our earlier study (Khurana et al., 2016). The antigenic regions/sites (8–247 amino acid residues) were defined based on antibody recognition by at least 4% of phage clones obtained after affinity selection with at least one plasma sample in this study or by the rVSV-EBOV GP vaccination-induced antibodies in the previous study. The frequency of phages expressing these GP antigenic sites selected by plasma following EBOV infection (Figure 3B) and ChAd3-MVA (Figure 3C) vaccination is shown (Table S2).

Importantly, EBOV infection (black, blue, red, and purple bars in Figure 3B) induced a more diverse anti-GP antibody response across both GP1 and GP2 that included antigenic sites I, III.2, IV.4, V.9 (fusion peptide), VI (C terminus of GP2), and VII that were preferentially recognized by post-infection survivor antibodies compared with post ChAd3-MVA vaccination plasma samples (pink and green bars in Figure 3C). Interestingly, the later (6 months) post-infection plasma (#28) contained antibodies that recognized two sites with high frequency in GP1 (III.1; GP 210–220 and V.6; GP 456–484) that were selected minimally by convalescent plasma at early time points post-EBOV infection (2 and 3 months post-infection) or the ChAd3-MVA post-vaccination-induced antibodies. However, it is possible that this may reflect different individuals rather than expanding repertoire. The ChAd3-MVA vaccination generated antibodies that primarily recognized antigenic sites in glycan cap (sites IV, IV.1, IV.2) and MLD (sites V.1 to V.8) in either the high (#58) or low (#64) neutralization titer plasma pool (Figure 3C). Post-infection samples #79 and #92 with the highest *in vitro* neutralization titer either in the classical PRNT or PsVN assay demonstrated immunodominance in the GP2 site (sites V.9, V.10, VI, and VII) binding antibodies (red and purple bars in Figure 3B). Antigenic sites V.5 (GP 436–491), V.11 (GP 439–465), and VII (GP 603–624) were recognized at higher frequency by plasma sample #92 compared with other survivor plasma (#28, #43 and #79) samples (Figure 3B and Table S2). This GFPDL analyses also identified nine novel antigenic sites (highlighted in red in Table S2) compared with the prior epitope profiling in the VSV-EBOV GP vaccination study, including sites II.3, III.2, III.3, IV.4, V.8, and V.11 in GP1, an immunodominant sequence (V.9) in the N-terminal part of GP2 near the fusion peptide and sites V.8, V.10, and VII in GP2.

## Post-EBOV Infection Survivor Plasma Shows Higher Antibody Binding to Diverse Antigenic Sites in GP Than Post-Vaccination Plasma

To follow up on antigenic sites identified using GFPDL analysis, peptides representing most of the unique antigenic sites up to 70 amino acid residues long were chemically synthesized and evaluated for individual samples antibody binding in SPR (Figure 4A and see Transparent Methods). The post-infection survivor

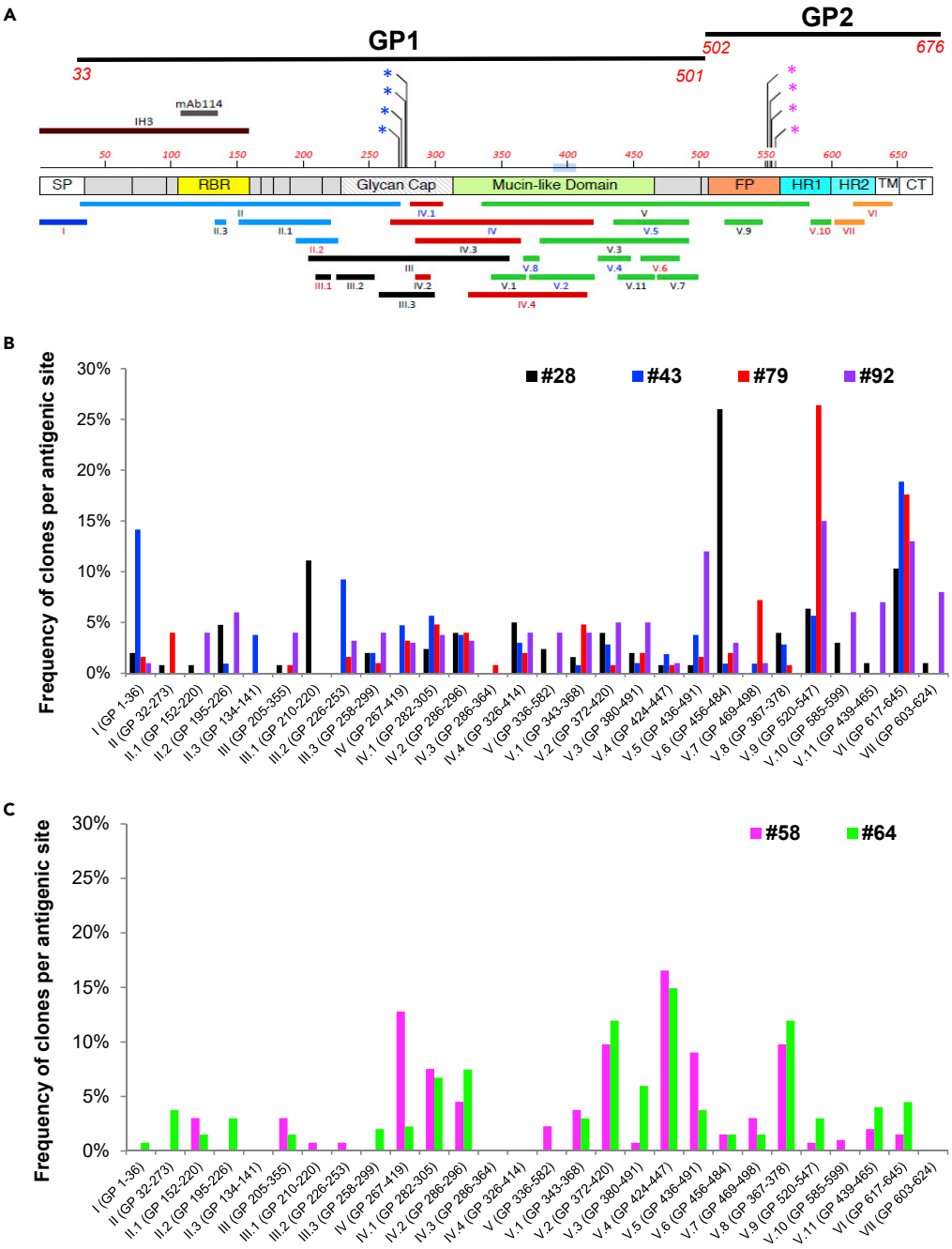


**Figure 3. Elucidation of Antibody Epitope Profile against the EBOV Glycoprotein following ChAd3-MVA Vaccination or EBOV Infection in Survivors**

(A) Antigenic sites within the EBOV-GP recognized by plasma antibodies following EBOV infection in survivors (based on data presented in Figure 2). The amino acid designation is based on the GP protein sequence encoded by the complete EBOV-GP gene (Figure S2). Previously described MAb epitopes in clinical trials are shown above the GP schematic. Critical residues for binding of MAbs in anti-EBOV cocktails, ZMapp (13C6, blue asterisks and 2G4 and 4G7, pink asterisks) and MAb 114, are depicted. The antigenic regions/sites discovered in this study using the post-infection and post-vaccination plasma antibodies are depicted below the GP schematic and are color coded.

(B and C) Distribution and frequency of phage clones expressing inserts spanning each of the key GP antigenic sites following EBOV infection (#28, black; #43, blue; #79, red; and #92, purple) in survivors (B) or vaccination (C) with ChAd3-MVA vaccine (#58, pink and #64, green). The number of clones that encoded for each antigenic site was divided by the total number of EBOV-GFPDL selected clones for each plasma and is represented as a percentage for two independent experiments.

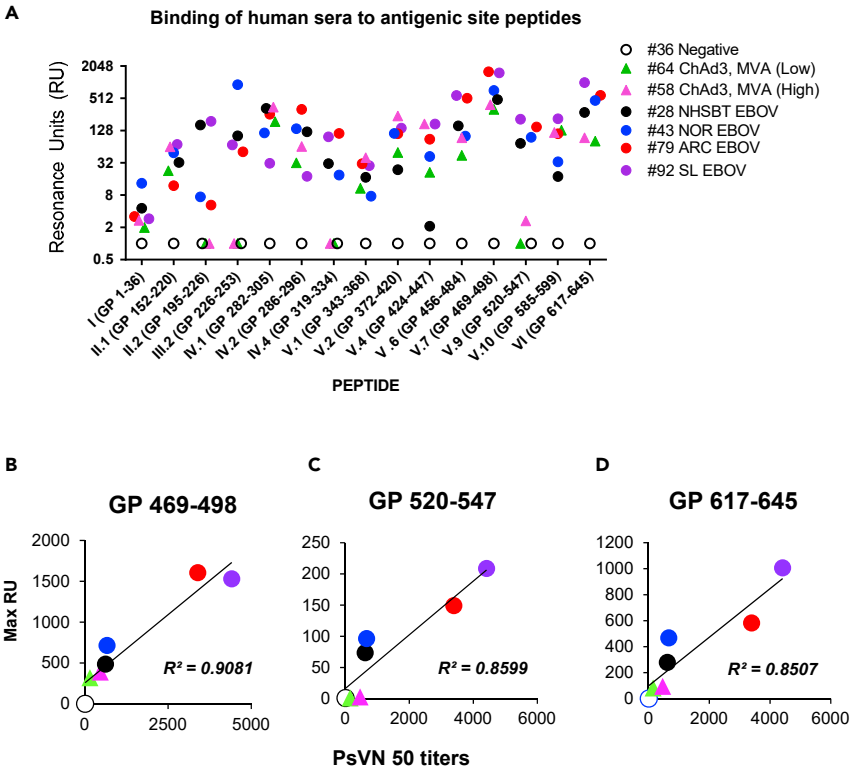


**Figure 4. Analysis of Human Plasma Binding to GFPDL-Identified GP Antigenic Site Peptides by SPR**

(A) Ten-fold dilution of plasma samples collected from EBOV survivors (#28, black; #43, blue; #79, red; and #92, purple) or humans vaccinated with ChAd3-MVA vaccine (#58, pink triangle and #64, green triangle) or mock control (#36, empty circle) were analyzed for total binding to chemically synthesized peptides containing the antigenic sites identified by GFPDL (Figure 3A) in SPR. Total antibody binding is represented in SPR resonance units.

(B–D) Total binding antibody (Max RU) of human plasma against antigenic site peptides (B) GP 469–498 (site V.7 in the C terminus of GP1), (C) GP 520–547 (site V.9 in fusion peptide at the N terminus of GP2), and (D) GP 617–645 (site VI in HR2-TM domain at the C terminus of GP2) correlated with the homologous virus neutralization (PsVN) titers. Pearson correlations are reported for the calculation of correlations between total anti-GP peptide antibody binding and PsVN titers.

samples (close circles) showed higher antibody binding to few antigenic site peptides compared with post-vaccination plasma (triangles), whereas for other sites, there was overlap in the extent of peptide binding by post-infectious and post-vaccination serum. The measured plasma sample reactivity against each peptide in SPR is possibly an aggregate sum of different antibodies recognizing overlapping epitopes in multiple antigenic sites (as defined by the GFPDL in Figures 2 and 3) contained in that peptide. Sites II.2 (GP 195–226), III.2 (GP 226–253), IV.4 (GP 319–334), and V.9 (GP 520–547) showed moderate/strong antibody binding only to post-infection samples with minimal or no binding with post-vaccination plasma antibodies (Figure 4A). EBOV survivor samples also showed 2-to 10-fold higher antibody binding to antigenic site in the C terminus of GP1 (site V.7; 469–498) and 5- to 20-fold higher binding for the C terminus of GP2 (site VI; 617–645). ChAd3-MVA vaccination induced comparable or modestly higher antibody binding to antigenic sites IV. (GP 282–305), V.2 (GP 372–420), V.4 (GP 424–447) in the MLD of GP1, and V.10 (GP 585–599) in the HR1 of GP2. Relationship analysis of antibody binding titers to each antigenic site peptide with PsVN titers showed a significant correlation of antibody binding to peptides GP 469–498 (site V.7 in the C terminus of GP1), GP 520–547 (site V.9 in fusion peptide at the N terminus of GP2), and GP 617–645 (site VI in HR2-TM domain at the C terminus of GP2) (Figures 4B–4D). In this specific case, it is quite interesting that individual survivors had a more diverse response than that seen in pooled vaccines.

In summary, this study demonstrated that EBOV infection induced a more diverse, durable, high-affinity IgG antibody response than vaccination using adenovirus/MVA vectors in terms of antibody epitope repertoire diversity, antibody isotype class switching, and antibody affinity in humans.

## DISCUSSION

A comprehensive understanding of the humoral immune response following EBOV infection and vaccination is required to identify immune markers that can provide protection to facilitate development and evaluation of effective vaccine candidates against lethal EVD. The main focus of this study was to identify the overall global pattern of antibody epitope fingerprint and antibody qualitative profile generated following human EBOV infection in survivor's versus vaccination. Since in this study the vaccinated sera were pooled from multiple individuals, all comparisons between vaccination versus EBOV infection reflect individual/pooled survivor samples with pooled ChAd3-MVA vaccinee samples.

EBOV infection in survivors generated a higher anti-GP-binding antibody titer compared with ChAd3-MVA prime boost-vaccination. The observed differences in neutralization between EVD survivor samples with low (#28 & #43) and high (#79 & #92) titer suggest that EVD survivors may generate a variable immune response following EBOV infection. The difference in neutralization antibody titers and/or potency may correlate with antibody affinity and specificity for higher frequency of antibody binding to the fusion peptides and base of the stalk in samples #79 and #92 compared with #28 and #43, as observed with MAbs from survivors (Bornholdt et al., 2016). Real-time antibody kinetics of post-vaccination antibodies by SPR revealed limited antibody class switching and modest antibody affinity even after prime-boost vaccination compared with post-infection antibodies in EBOV survivors even with a similar timescale following vaccination/infection. The ChAd3-MVA (replication-defective) vaccination-induced antibody class switching and affinity was similar to that generated by rVSV-EBOV-GP (a replication competent virus) vaccination in our previous study (Khurana et al., 2016). Importantly, the GP-binding antibodies induced by EBOV infection were long-lasting responses, lasting up to 6 months post-infection, in contrast to the rVSV-EBOV GP prime-boost vaccination study that demonstrated a short-lived antibody response, which declined to pre-vaccination levels by 6 months post-vaccination (Khurana et al., 2016). Moreover, the presence of GP-bound IgG4 in most survivor plasma suggests a persistent infection or long-term exposure to antigen following EBOV infection. Since IgG2 response is mostly driven by polysaccharide antigens, an IgG2 response of 8.3% GP-binding antibodies in sample #92 obtained from six EVD survivors in Sierra Leone (who did not receive any experimental treatment) is speculated to be due to a possible polysaccharide antigen-induced class switching to IgG2 by highly glycosylated GP following infection.

Although the numbers of captured GFPDL phages following ChAd3-MVA vaccination were comparable with those generated following infection, the antibody epitope repertoire generated following EBOV infection in survivors showed greater diversity compared with ChAd3-MVA prime-boost vaccination-induced antibody response. It is possible that the more focused response to vector-GP vaccination is due to the limited (one round) vector replication that only produces GP once inside a cell compared with productive EBOV infection that can stimulate the immune system over a prolonged period. Importantly, both high- (#58) and low- (#64) titer post-vaccination samples (based on the *in vitro* neutralization data) recognized similar antibody epitope diversity that was skewed toward the glycan cap and MLD of GP1, whereas the post-infection plasma samples demonstrated strong antibody binding to C-terminal parts of GP1 and GP2. This ChAd3-MVA prime-boost vaccination-induced antibody response contrasts with the replication competent rVSV-EBOV GP vaccine, which showed a more diverse antibody repertoire with antibody binding to GP2 as previously reported (Khurana et al., 2016). These findings suggest that ChAd3-MVA prime boost vaccination should be further optimized to generate a more diverse antibody repertoire.

Three of the four EVD survivors who donated plasma for the current study received immunological treatments such as ZMapp (#43) or convalescent plasma (# 28 and #79), and it is possible that the antibody composition in their blood could have been influenced by the antibody treatments, despite the time interval between the onset of disease and donation of the plasma (2–6 months post-infection). Antibodies to viral proteins in addition to GP were observed in immunoblots indicating that antibodies resulting from EBOV infection were present in these survivor's plasma (Wilkinson et al., 2017). Plasma pool #92 obtained from six Sierra Leone survivors who did not receive any experimental treatment showed an overall similar epitope repertoire as other survivors; however, it recognized antigenic sites V.5 (GP 436–491), V.11 (GP 439–465), and VII (GP 603–624) at a higher frequency compared with other survivor plasma samples (#28, #43, and #79). It is possible that antibody treatment (ZMapp or convalescent plasma) of patients (#28, #43, and #79) may have altered some specific epitopes in #28, #43, and #79 that were recognized by the Sierra Leone patients (#92) who did not receive any Ebola-specific antibody treatment, even though patients' immune systems would have seen virus for a number of days before the patients were treated.

GFPDL identified several overlapping antigenic sites like sites V.6 and V.7 (Table S2). Site V.6 shows high frequency in #28 and minimally in other survivor samples including those sampled at earlier time points (#43 and #79), whereas site V.7 is preferentially recognized by antibodies in sample #43 but not by sample #28. However, peptides representing both antigenic sites show good antibody binding with all survivor samples in SPR indicating antibodies recognizing epitopes in these overlapping antigenic sites (Figure 4). Survivor sample #43 (2 months post-infection) who received ZMapp treatment (and not convalescent plasma) demonstrated a diverse antibody epitope repertoire similar to that of samples #28 and #79 who received convalescent plasma treatment. Moreover, ZMapp MAb cocktail does not contain antibodies that recognize sites VI in the C terminus of GP2, which was preferentially recognized by all post-infection survivor samples. However, this finding for preferential binding of antibodies to the C terminus of GP2 following EBOV infection needs to be further evaluated in a larger number of Ebola patients.

A possible limitation of GFPDL-based assessments is that they are unlikely to detect rare quaternary epitopes that cross GP protomers or epitopes with post-translational modification. However, in earlier studies, GFPDL was used to identify conformation-dependent epitopes of neutralizing and protective MAbs. Moreover, ~90% of anti-GP antibodies from high-titer post-infection survivor plasma were removed by adsorption with our EBOV GP GFPDL, supporting the use of the EBOV GP GFPDL for analyses of human antibody repertoire, as was also observed previously with other viral antigens including different Influenza strains, RSV-F, and heavily glycosylated RSV-G (Fuentes et al., 2016; Khurana et al., 2009, 2010, 2011b). Use of SPR with the glycosylated EBOV GP overcomes these limitations and provides additional insight into the anti-GP polyclonal antibody response following vaccination or infection. The SPR approach is species independent and captures all antibody classes including IgM, IgA, and IgG and is also more appropriate for maintaining the native structure of the EBOV GP and preservation of conformational epitopes. The antigenic fingerprinting provides an overall global pattern of antibody epitope specificities generated following Ebola vaccination versus infection in humans. This study should be expanded to additional samples from vaccinees and EBOV-infected individuals from ongoing and previous Ebola outbreaks in different populations to evaluate the contribution of MHC haplotype and so epitope reactivity for individual samples to make firm conclusions.

Antibody binding of human plasma samples to the three antigenic site peptides (GP 469–498 at the C terminus of GP1, GP 520–547 in the fusion peptide, and GP 617–645 in the GP2-HR2 domain) that showed a strong correlation with neutralization titers possibly indicates an important role of antibodies to these sites in protection against EBOV infection and disease *in vivo*. Although non-neutralizing antibodies may be protective *in vivo*, preliminary data from recent clinical trial in the DRC have demonstrated that neutralizing antibodies like MAb 114 may provide better clinical outcome associated with significantly reduced mortality (Kupferschmidt, 2019).

Altogether, our study demonstrated a different antigenic fingerprint following EBOV infection in survivors compared with a live ChAd3-MVA non-replication vector-based vaccine in terms of antibody epitope repertoire diversity, antibody isotype class switching, and antibody affinity. This contributes to a better understanding of quantitative and qualitative aspects of immune responses that could aid development and evaluation of effective EBOV therapeutics and vaccines.

### Limitations of the Study

A possible limitation of GFPDL-based assessments is that they are unlikely to detect rare quaternary epitopes that cross GP protomers or epitopes that require post-translational modification. Second, this study should be expanded to testing of additional individual samples at different time points following vaccination/infection from vaccinees and EBOV-infected individuals from ongoing and previous Ebola outbreaks in different populations to make firm conclusions.

## ETHICS STATEMENT

The study at CBER, FDA was conducted with de-identified samples under Research Involving Human Subjects (RIHSC) exemption #15-0B, and all assays performed fell within the permissible usages in the original consent.

## METHODS

All methods can be found in the accompanying Transparent Methods supplemental file.

## DATA AND CODE AVAILABILITY

Further information and requests for resources and reagents should be directed to the Lead Contact, Surender Khurana (Surender.Khurana@fda.hhs.gov). There are restrictions to the availability of the GFPDL technology and Ebola peptides described in this study due to US patent application.

## SUPPLEMENTAL INFORMATION

Supplemental Information can be found online at https://doi.org/10.1016/j.isci.2020.100920.

## ACKNOWLEDGMENTS

We thank S. Rubin and H. Golding for their insightful review of the manuscript. We thank NIBSC (D. Wilkinson) for providing the clinical samples as part of a WHO study. Source materials for the WHO study were donated by Teresa Lambe, Sarah Gilbert, Adrian Hill, and Katie Ewer (Jenner Institute, University of Oxford, UK); Annie Winkler (Emory University, USA); Scott Koepsell (University of Nebraska); Arne Brantsaeter, Richard Olaussen, Unni Bergerud (Oslo University Hospital); Sheila MacLennan, Alex Barber (National Health Service Blood and Transplant, Leeds, UK), and Calum Semple (University of Liverpool, UK). The antibody characterization work described in this manuscript was supported by US Food and Drug Administration (FDA) Office of Counterterrorism and Emerging Threats (OCET) - Medical Countermeasures initiative (MCMi) OCET 2019-1018 funds to S.K. The funders had no role in study design, data collection and analysis, decision to publish, or preparation of the manuscript. The content of this publication does not necessarily reflect the views or policies of the Department of Health and Human Services, nor does mention of trade names, commercial products, or organizations imply endorsement by the US Government.

## AUTHOR CONTRIBUTIONS

Designed research: S.K.; Performed research – S.F., S.R., E.M.C., L.K, and S.K.; Contributed to Writing – S.K.

## DECLARATION OF INTERESTS

The authors have declared that no competing interests exist. The GFPDL technology and Ebola peptides described in this study are covered by US patents.

Received: June 3, 2019
Revised: January 14, 2020
Accepted: February 12, 2020
Published: March 27, 2020

## REFERENCES

Blaney, J.E., Marzi, A., Willet, M., Papaneri, A.B., Wirblich, C., Feldmann, F., Holbrook, M., Jahrling, P., Feldmann, H., and Schnell, M.J. (2013). Antibody quality and protection from lethal Ebola virus challenge in nonhuman primates immunized with rabies virus based bivalent vaccine. PLoS Pathog. *9*, e1003389.

Bornholdt, Z.A., Turner, H.L., Murin, C.D., Li, W., Sok, D., Souders, C.A., Piper, A.E., Goff, A., Shamblin, J.D., Wollen, S.E., et al. (2016). Isolation of potent neutralizing antibodies from a survivor of the 2014 Ebola virus outbreak. Science *351*, 1078–1083.

Crook, P., Smith-Palmer, A., Maguire, H., McCarthy, N., Kirkbride, H., Court, B., Kanagarajah, S., Turbitt, D., Ahmed, S., Cosford, P., et al. (2017). Lack of secondary transmission of ebola virus from healthcare worker to 238 contacts, United Kingdom, December 2014. Emerg. Infect. Dis. *23*, 2081–2084.

Dye, J.M., Herbert, A.S., Kuehne, A.I., Barth, J.F., Muhammad, M.A., Zak, S.E., Ortiz, R.A., Prugar, L.I., and Pratt, W.D. (2012). Postexposure antibody prophylaxis protects nonhuman primates from filovirus disease. Proc. Natl. Acad. Sci. U S A *109*, 5034–5039.

Ewer, K., Rampling, T., Venkatraman, N., Bowyer, G., Wright, D., Lambe, T., Imoukhuede, E.B., Payne, R., Fehling, S.K., Strecker, T., et al. (2016). A monovalent chimpanzee adenovirus ebola vaccine boosted with MVA. N. Engl. J. Med. *374*, 1635–1646.

Fuentes, S., Coyle, E.M., Beeler, J., Golding, H., and Khurana, S. (2016). Antigenic fingerprinting following primary RSV infection in young children identifies novel antigenic sites and reveals unlinked evolution of human antibody repertoires to fusion and attachment glycoproteins. PLoS Pathog. *12*, e1005554.

Fuentes, S., Ravichandran, S., and Khurana, S. (2018). Antibody repertoire of human polyclonal antibodies against ebola virus glycoprotein generated after deoxyribonucleic acid and protein vaccination of transchromosomal bovines. J. Infect. Dis. *218*, S597–S602.

Henao-Restrepo, A.M., Longini, I.M., Egger, M., Dean, N.E., Edmunds, W.J., Camacho, A., Carroll, M.W., Doumbia, M., Draguez, B., Duraffour, S., et al. (2015). Efficacy and effectiveness of an rVSV-vectored vaccine expressing Ebola surface glycoprotein: interim results from the Guinea ring vaccination cluster-randomised trial. Lancet *386*, 857–866.

Holtsberg, F.W., Shulenin, S., Vu, H., Howell, K.A., Patel, S.J., Gunn, B., Karim, M., Lai, J.R., Frei, J.C., Nyakatura, E.K., et al. (2015). Pan-ebolavirus and pan-filovirus mouse monoclonal antibodies: protection against Ebola and Sudan viruses. J. Virol. *90*, 266–278.

Jones, S.M., Feldmann, H., Stroher, U., Geisbert, J.B., Fernando, L., Grolla, A., Klenk, H.D., Sullivan, N.J., Volchkov, V.E., Fritz, E.A., et al. (2005). Live attenuated recombinant vaccine protects nonhuman primates against Ebola and Marburg viruses. Nat. Med. *11*, 786–790.

Kanapathipillai, R., Henao Restrepo, A.M., Fast, P., Wood, D., Dye, C., Kieny, M.P., and Moorthy, V. (2014). Ebola vaccine–an urgent international priority. N. Engl. J. Med. *371*, 2249–2251.

Kennedy, S.B., Bolay, F., Kieh, M., Grandits, G., Badio, M., Ballou, R., Eckes, R., Feinberg, M., Follmann, D., Grund, B., et al. (2017). Phase 2 placebo-controlled trial of two vaccines to prevent ebola in Liberia. N. Engl. J. Med. *377*, 1438–1447.

Khurana, S., Needham, J., Mathieson, B., Rodriguez-Chavez, I.R., Catanzaro, A.T., Bailer, R.T., Kim, J., Polonis, V., Cooper, D.A., Guerin, J., et al. (2006). Human immunodeficiency virus (HIV) vaccine trials: a novel assay for differential diagnosis of HIV infections in the face of vaccine-generated antibodies. J. Virol. *80*, 2092–2099.

Khurana, S., Suguitan, A.L., Jr., Rivera, Y., Simmons, C.P., Lanzavecchia, A., Sallusto, F., Manischewitz, J., King, L.R., Subbarao, K., and Golding, H. (2009). Antigenic fingerprinting of H5N1 avian influenza using convalescent sera and monoclonal antibodies reveals potential vaccine and diagnostic targets. PLoS Med. *6*, e1000049.

Khurana, S., Chearwae, W., Castellino, F., Manischewitz, J., King, L.R., Honorkiewicz, A., Rock, M.T., Edwards, K.M., Del Giudice, G., Rappuoli, R., et al. (2010). Vaccines with MF59 adjuvant expand the antibody repertoire to target protective sites of pandemic avian H5N1 influenza virus. Sci. Transl. Med. *2*, 15ra15.

Khurana, S., Sasono, P., Fox, A., Nguyen, V.K., Le, Q.M., Pham, Q.T., Nguyen, T.H., Nguyen, T.L., Horby, P., and Golding, H. (2011a). H5N1-SeroDetect EIA and rapid test: a novel differential diagnostic assay for serodiagnosis of H5N1 infections and surveillance. J. Virol. *85*, 12455–12463.

Khurana, S., Verma, N., Yewdell, J.W., Hilbert, A.K., Castellino, F., Lattanzi, M., Del Giudice, G., Rappuoli, R., and Golding, H. (2011b). MF59 adjuvant enhances diversity and affinity of antibody-mediated immune response to pandemic influenza vaccines. Sci. Transl. Med. *3*, 85ra48.

Khurana, S., Fuentes, S., Coyle, E.M., Ravichandran, S., Davey, R.T., Jr., and Beigel, J.H. (2016). Human antibody repertoire after VSV-Ebola vaccination identifies novel targets and virus-neutralizing IgM antibodies. Nat. Med. *22*, 1439–1447.

Khurana, S., Hahn, M., Coyle, E.M., King, L.R., Lin, T.L., Treanor, J., Sant, A., and Golding, H. (2019). Repeat vaccination reduces antibody affinity maturation across different influenza vaccine platforms in humans. Nat. Commun. *10*, 3338.

Krause, P.R. (2015). Interim results from a phase 3 Ebola vaccine study in Guinea. Lancet *386*, 831–833.

Kupferschmidt, K. (2019). Successful Ebola treatments promise to tame outbreak. Science *365*, 628–629.

Lee, J., Klenow, L., Coyle, E.M., Golding, H., and Khurana, S. (2018). Protective antigenic sites in respiratory syncytial virus G attachment protein outside the central conserved and cysteine noose domains. PLoS Pathog. *14*, e1007262.

Marzi, A., Engelmann, F., Feldmann, F., Haberthur, K., Shupert, W.L., Brining, D., Scott, D.P., Geisbert, T.W., Kawaoka, Y., Katze, M.G., et al. (2013). Antibodies are necessary for rVSV/ZEBOV-GP-mediated protection against lethal Ebola virus challenge in nonhuman primates. Proc. Natl. Acad. Sci. U S A *110*, 1893–1898.

Marzi, A., Feldmann, F., Geisbert, T.W., Feldmann, H., and Safronetz, D. (2015a). Vesicular stomatitis virus-based vaccines against Lassa and Ebola viruses. Emerg. Infect. Dis. *21*, 305–307.

Marzi, A., Robertson, S.J., Haddock, E., Feldmann, F., Hanley, P.W., Scott, D.P., Strong, J.E., Kobinger, G., Best, S.M., and Feldmann, H. (2015b). EBOLA VACCINE. VSV-EBOV rapidly protects macaques against infection with the 2014/15 Ebola virus outbreak strain. Science *349*, 739–742.

Matassov, D., Marzi, A., Latham, T., Xu, R., Ota-Setlik, A., Feldmann, F., Geisbert, J.B., Mire, C.E., Hamm, S., Nowak, B., et al. (2015). Vaccination with a highly attenuated recombinant vesicular stomatitis virus vector protects against challenge with a lethal dose of ebola virus. J. Infect. Dis. *212* (*Suppl 2*), S443–S451.

Mate, S.E., Kugelman, J.R., Nyenswah, T.G., Ladner, J.T., Wiley, M.R., Cordier-Lassalle, T., Christie, A., Schroth, G.P., Gross, S.M., Davies-Wayne, G.J., et al. (2015). Molecular evidence of sexual transmission of ebola virus. N. Engl. J. Med. *373*, 2448–2454.

Milligan, I.D., Gibani, M.M., Sewell, R., Clutterbuck, E.A., Campbell, D., Plested, E., Nuthall, E., Voysey, M., Silva-Reyes, L., McElrath, M.J., et al. (2016). Safety and immunogenicity of novel adenovirus type 26- and modified vaccinia ankara-vectored ebola vaccines: a randomized clinical trial. JAMA *315*, 1610–1623.

Rampling, T., Ewer, K., Bowyer, G., Wright, D., Imoukhuede, E.B., Payne, R., Hartnell, F., Gibani, M., Bliss, C., Minhinnick, A., et al. (2016). A monovalent chimpanzee adenovirus ebola vaccine - preliminary report. N. Engl. J. Med. *374*, 1635–1646.

Regules, J.A., Beigel, J.H., Paolino, K.M., Voell, J., Castellano, A.R., Munoz, P., Moon, J.E., Ruck, R.C., Bennett, J.W., Twomey, P.S., et al. (2017). A recombinant vesicular stomatitis virus ebola vaccine - preliminary report. N. Engl. J. Med. *376*, 330–341.

Ruibal, P., Oestereich, L., Ludtke, A., Becker-Ziaja, B., Wozniak, D.M., Kerber, R., Korva, M., Cabeza-Cabrerizo, M., Bore, J.A., Koundouno, F.R., et al. (2016). Unique human immune signature of Ebola virus disease in Guinea. Nature *533*, 100–104.

Tapia, M.D., Sow, S.O., Lyke, K.E., Haidara, F.C., Diallo, F., Doumbia, M., Traore, A., Coulibaly, F., Kodio, M., Onwuchekwa, U., et al. (2016). Use of ChAd3-EBO-Z Ebola virus vaccine in Malian and US adults, and boosting of Malian adults with MVA-BN-Filo: a phase 1, single-blind, randomised trial, a phase 1b, open-label and double-blind, dose-escalation trial, and a nested, randomised, double-blind, placebo-controlled trial. Lancet Infect. Dis. *16*, 31–42.

Wilkinson, D.E., Page, M., Mattiuzzo, G., Hassall, M., Dougall, T., Rigsby, P., Stone, L., and Minor, P. (2017). Comparison of platform technologies for assaying antibody to Ebola virus. Vaccine *35*, 1347–1352.

Wong, G., Richardson, J.S., Pillet, S., Patel, A., Qiu, X., Alimonti, J., Hogan, J., Zhang, Y., Takada, A., Feldmann, H., et al. (2012). Immune parameters correlate with protection against ebola virus infection in rodents and nonhuman primates. Sci. Transl. Med. *4*, 158ra146.

**iScience, Volume *23***

## Supplemental Information

# Human Antibody Repertoire following Ebola Virus Infection and Vaccination

**Sandra Fuentes, Supriya Ravichandran, Elizabeth M. Coyle, Laura Klenow, and Surender Khurana**

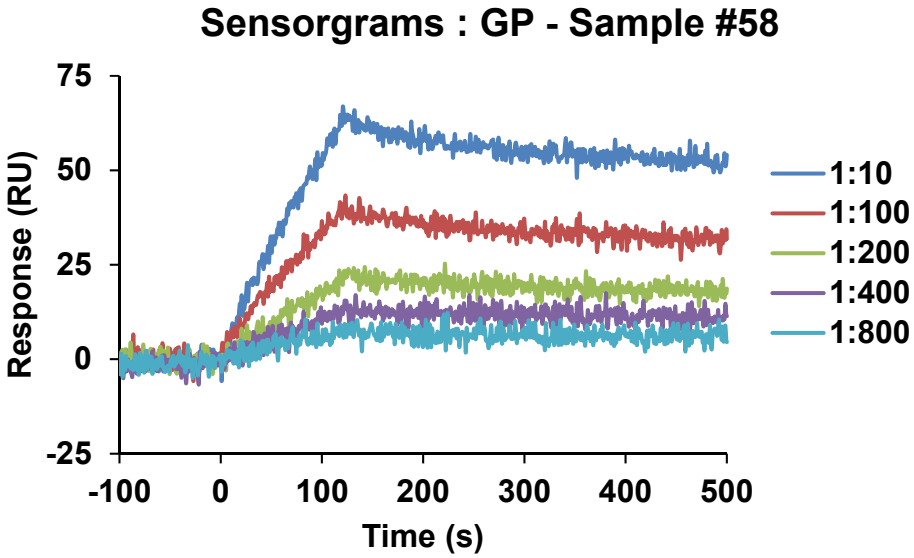


**Figure S1**

**Steady-state equilibrium analysis of different dilutions of plasma antibodies binding to Makona GP by SPR. Related to Figure 1.** Serial dilutions of plasma samples were injected simultaneously onto both Makona GP immobilized on a GLC sensor chip and on a surface free of protein (used as a blank). Binding was recorded using BioRad Proteon surface plasmon resonance biosensor instrument. Responses from the protein surface were corrected for the response from the mock surface and for responses from a separate, buffer only injection. Antibody off-rate constants, which describe the fraction of antigen-antibody complexes that decay per second, were determined directly from the plasma sample interaction with GP using SPR in the dissociation phase only for the sensorgrams with Max RU in the range of 10-100 RU and calculated using the BioRad ProteOn manager software for the heterogeneous sample model


**Figure S2: Related to Figure 2.** Complete EBOV-Makona GP gene translated sequence used for construction of EBOV-GFPD library and depiction in Figure 2 – 3.

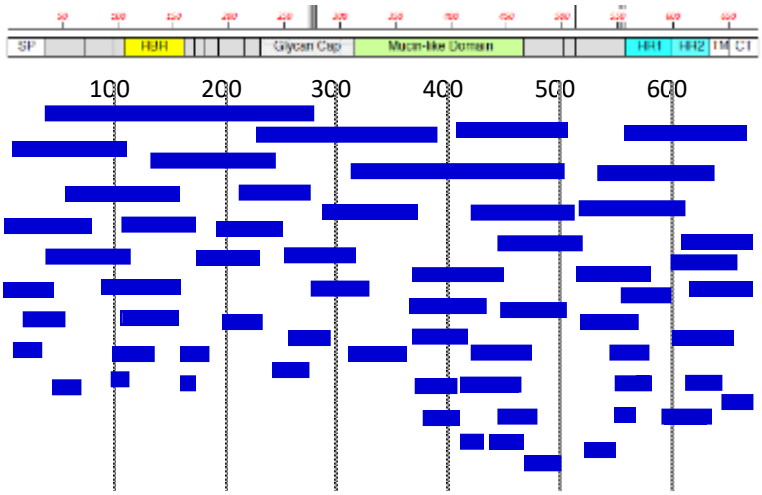


**Figure S3: Random distribution of size and sequence of the EBOV-GFPDL**. **Related to Figure 2.** Sequencing of Makona (2014) GP fragments expressed by the phages of the EBOV GFPD libraries were aligned to the Makona (2014) GP translated sequence (shown in Supplementary figure 2).

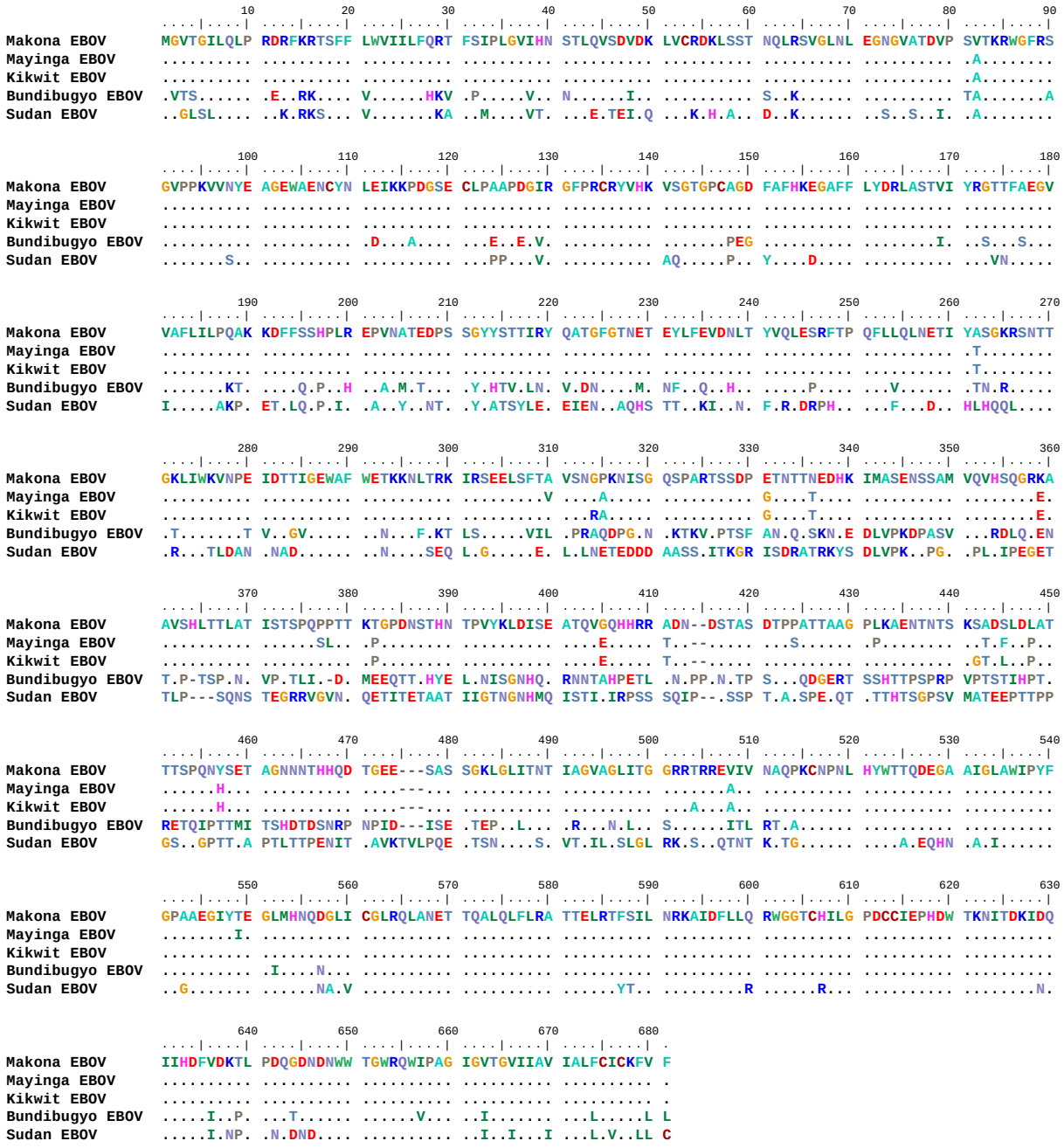


**Figure S4: Related to Figures 2 and 4.** Alignment of glycoprotein (GP) sequences from EBOV Makona (2014), Mayinga (1976), Kikwit (1995), Bundibugyo and Sudan strains.

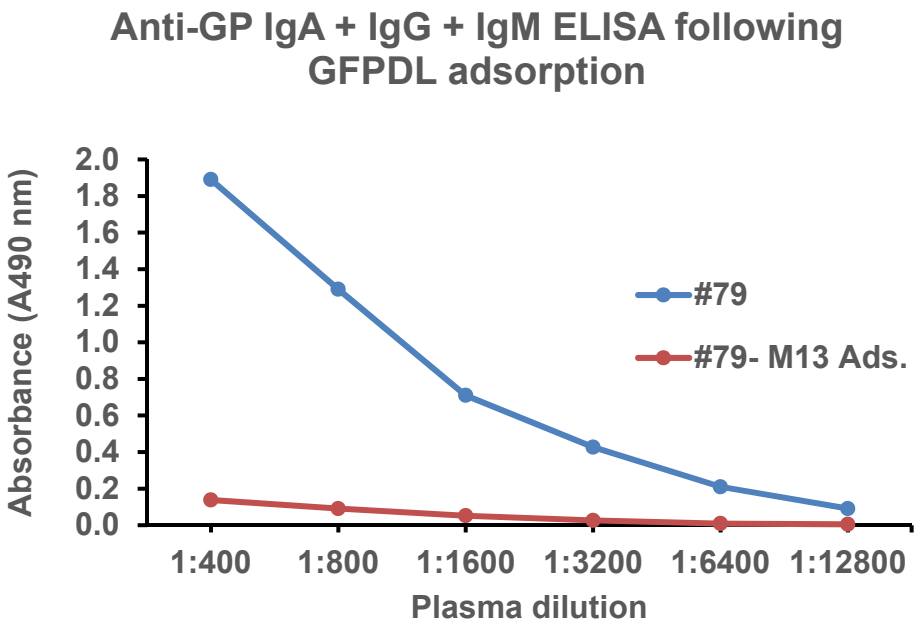


**Figure S5: Anti-GP reactivity of EBOV convalescent plasma in ELISA before and after EBOV-GFPDL adsorption. Related to Figure 2.** Post EBOV infected convalescent plasma #79 was adsorbed on Makona GFPDL coated petri dishes. Binding to recombinant EBOV-GP is shown before (solid purple line) and after (dashed purple line) GFPDL-adsorption in ELISA using HRP-conjugated goat anti-human IgA + IgG + IgM specific antibody.

**Table S1: Plasma Samples used in the Study. Related to Figures 1-4.**

| Sample Code | Sample Name | PRNT | PsVN |
|---|---|---|---|
| **#36 Negative** | **NHSBT EBOV Ab Negative Plasma** | <10 | <20 |
| **#64 ChAd3, MVA (Low)** | **VACCINEES PLASMA POOL (LOW)** Prime: ChAd3–vectored EBOV Mayinga GP Boost: MVA-vectored EBOV Mayinga GP, Sudan ebolavirus GP, Marburgvirus GP and Tai Forest nucleoprotein | NT | 157 |
| **#58 ChAd3, MVA (High)** | **VACCINEES PLASMA POOL (HIGH)** Prime: ChAd3–vectored EBOV Mayinga GP Boost: MVA-vectored EBOV Mayinga GP, Sudan ebolavirus GP, Marburgvirus GP and Tai Forest nucleoprotein | NT | 469 |
| **#28 NHSBT EBOV** | **NHSBT EBOV CONVALESCENT AB** Brincidifovar (anti-viral) and convalescent plasma treatments- 6 months post infection sample | 45 | 623 |
| **#43 NOR EBOV** | **NORWEGIAN EBOV CONVALESCENT AB** ZMAb (anti-GP), Favipiravin (RNA pol inhibitor) and TKM-100802 (iRNA), 2 month post infection sample | 27 | 669 |
| **#79 ARC EBOV** | **AMERICAN RED CROSS EBOV CONVALESCENT AB** 2 aliquots of convalescent plasma 24 hours apart as well as 7 nightly infusions of TKM-Ebola (iRNA), No Mab. 3 months post-infection sample. | 181 | 3395 |
| **#92 SL EBOV** | **SIERRA LEONE EBOV CONVALESCENT AB** Pooled convalescent plasma of six patients who recovered from EVD are likely to not have received any Ebola-specific treatment. | 512 | 4414.5 |

NT - Sample not tested:

**Table S2: Antigenic sites and frequency of sites in Plasma samples. Related to Figures 2-4.**

| Site | AA | Sequence | Post Infection | | | | Post Vaccination | |
|---|---|---|---|---|---|---|---|---|
| | | | #28 | #43 | #79 | #92 | #58 | #64 |
| I | 1-36 | MGVTGILQLPRDRFKRTSFFLWVIILFQRTFSIPLG | 2% | 14% | 2% | 1% | 0% | 1% |
| II | 32-273 | SIPLGVIHNSTLQVSDVDKLVCRDKLSSTNQLRSVGLNLEGNGV ATDVPSVTKRWGFRSGVPPKVVNYEAGEWAENCYNLEIKKPD GSECLPAAPDGIRGFPRCRYVHKVSGTGPCAGDFAFHKEGAFF LYDRLASTVIYRGTTFAEGVVAFLILPQAKKDFFSSHPLREPVNA TEDPSSGYYSTTIRYQATGFGTNETEYLFEVDNLTYVQLESRFT PQFLLQLNETIYASGKRSNTTGKL | 1% | 0% | 4% | 0% | 0% | 4% |
| II.1 | 152-220 | AFHKEGAFFLYDRLASTVIYRGTTFAEGVVAFLILPQAKKDFFSS HPLREPVNATEDPSSGYYSTTIRY | 1% | 0% | 0% | 4% | 3% | 1% |
| II.2 | 195-226 | SSHPLREPVNATEDPSSGYYSTTIRYQATGFG | 5% | 1% | 0% | 6% | 0% | 3% |
| II.3 | 134-141 | RCRYVHKV | 0% | 4% | 0% | 0% | 0% | 0% |
| III | 205-355 | ATEDPSSGYYSTTIRYQATGFGTNETEYLFEVDNLTYVQLESRF TPQFLLQLNETIYASGKRSNTTGKLIWKVNPEIDTTIGEWAFWET KKNLTRKIRSEELSFTAVSNGPKNISGQSPARTSSDPETNTTNE DHKIMASENSSAMVQVHS | 1% | 0% | 1% | 4% | 3% | 1% |
| III.1 | 210-220 | SSGYYSTTIRY | 11% | 0% | 0% | 0% | 1% | 0% |
| III.2 | 226-253 | GTNETEYLFEVDNLTYVQLESRFTPQFL | 0% | 9% | 2% | 3% | 1% | 0% |
| III.3 | 258-299 | ETIYASGKRSNTTGKLIWKVNPEIDTTIGEWAFWETKKNLTR | 2% | 2% | 1% | 4% | 0% | 2% |
| IV | 267-419 | SNTTGKLIWKVNPEIDTTIGEWAFWETKKNLTRKIRSEELSFTAV SNGPKNISGQSPARTSSDPETNTTNEDHKIMASENSSAMVQVH SQGRKAAVSHLTTLATISTSPQPPTTKTGPDNSTHNTPVYKLDI SEATQVGQHHRRADNDSTASD | 0% | 5% | 3% | 3% | 13% | 2% |
| IV.1 | 282-305 | DTTIGEWAFWETKKNLTRKIRSEE | 2% | 6% | 5% | 4% | 8% | 7% |
| IV.2 | 286-296 | GEWAFWETKKN | 4% | 4% | 4% | 3% | 5% | 7% |
| IV.3 | 286-364 | GEWAFWETKKNLTRKIRSEELSFTAVSNGPKNISGQSPARTSS DPETNTTNEDHKIMASENSSAMVQVHSQGRKAAVSH | 0% | 0% | 1% | 0% | 0% | 0% |
| IV.4 | 326-414 | TSSDPETNTTNEDHKIMASENSSAMVQVHSQGRKAAVSHLTTL ATISTSPQPPTTKTGPDNSTHNTPVYKLDISEATQVGQHHRRAD ND | 5% | 3% | 2% | 4% | 0% | 0% |
| V | 336-582 | NEDHKIMASENSSAMVQVHSQGRKAAVSHLTTLATISTSPQPP TTKTGPDNSTHNTPVYKLDISEATQVGQHHRRADNDSTASDTP PATTAAGPLKAENTNTSKSADSLDLATTTSPQNYSETAGNNNT HHQDTGEESASSGKLGLITNTIAGVAGLITGGRRTRREVIVNAQ PKCNPNLHYWTTQDEGAAIGLAWIPYFGPAAEGIYTEGLMHNQ DGLICGLRQLANETTQALQLFLRATTELRTF | 2% | 0% | 0% | 4% | 2% | 0% |
| V.1 | 343-368 | ASENSSAMVQVHSQGRKAAVSHLTTL | 2% | 1% | 5% | 4% | 4% | 3% |
| V.2 | 372-420 | STSPQPPTTKTGPDNSTHNTPVYKLDISEATQVGQHHRRADND STASDT | 4% | 3% | 1% | 5% | 10% | 12% |
| V.3 | 380-491 | TKTGPDNSTHNTPVYKLDISEATQVGQHHRRADNDSTASDTPP ATTAAGPLKAENTNTSKSADSLDLATTTSPQNYSETAGNNNTH HQDTGEESASSGKLGLITNTIAGVAG | 2% | 1% | 2% | 5% | 1% | 6% |
| V.4 | 424-447 | TTAAGPLKAENTNTSKSADSLDLA | 1% | 2% | 1% | 1% | 17% | 15% |
| V.5 | 436-491 | NTNTSKSADSLDLATTTSPQNYSETAGNNNTHHQDTGEESASS GKLGLITNTIAGVAG | 1% | 4% | 2% | 12% | 9% | 4% |
| V.6 | 456-484 | SETAGNNNTHHQDTGEESASSGKLGLITN | 26% | 1% | 2% | 3% | 2% | 1% |
| V.7 | 469-498 | TGEESASSGKLGLITNTIAGVAGLITGGRR | 0% | 1% | 7% | 1% | 3% | 1% |
| V.8 | 367-378 | TLATISTSPQPP | 4% | 3% | 1% | 0% | 10% | 12% |
| V.9 | 520-547 | TQDEGAAIGLAWIPYFGPAAEGIYTEGL | 6% | 6% | 26% | 15% | 1% | 3% |
| V.10 | 585-599 | LNRKAIDFLLQRWGG | 3% | 0% | 0% | 6% | 1% | 0% |
| V.11 | 439-465 | KSADSLDLATTTSPQNYSETAGNNNTH | 1% | 0% | 0% | 7% | 2% | 4% |
| VI | 617-645 | KNITDKIDQIIHDFVDKTLPDQGDNDNWW | 10% | 19% | 18% | 13% | 2% | 4% |
| VII | 603-624 | ILGPDCCIEPHDWTKNITDKID | 1% | 0% | 0% | 8% | 0% | 0% |

**Table S3: Sequence similarity of GP antigenic sites with other Ebola strains. Related to Figures 2-4.**

| Site | AA | Sequence | Makona (%) | Mayinga(%) | Kikwit(%) | Bundibugyo(%) | Sudan(%) |
|---|---|---|---|---|---|---|---|
| I | 1-36 | MGVTGILQLPRDRFKRTSFFLWVIILFQRTFSIPLG | 100 | 100 | 100 | 69.4 | 66.6 |
| II | 32-273 | SIPLGVIHNSTLQVSDVDKLVCRDKLSSTNQLRSVGLN LEGNGVATDVPSVTKRWGFRSGVPPKVVNYEAGEW AENCYNLEIKKPDGSECLPAAPDGIRGFPRCRYVHKV SGTGPCAGDFAFHKEGAFFLYDRLASTVIYRGTTFAE GVVAFLILPQAKKDFFSSHPLREPVNATEDPSSGYYS TTIRYQATGFGTNETEYLFEVDNLTYVQLESRFTPQFL LQLNETIYASGKRSNTTGKL | 100 | 99.1 | 99.1 | 80.1 | 68.1 |
| II.1 | 152-220 | AFHKEGAFFLYDRLASTVIYRGTTFAEGVVAFLILPQA KKDFFSSHPLREPVNATEDPSSGYYSTTIRY | 100 | 100 | 100 | 75.3 | 65.2 |
| II.2 | 195-226 | SSHPLREPVNATEDPSSGYYSTTIRYQATGFG | 100 | 100 | 100 | 53.1 | 43.7 |
| II.3 | 134-141 | RCRYVHKV | 100 | 100 | 100 | 100 | 87.5 |
| III | 205-355 | ATEDPSSGYYSTTIRYQATGFGTNETEYLFEVDNLTYV QLESRFTPQFLLQLNETIYASGKRSNTTGKLIWKVNPE IDTTIGEWAFWETKKNLTRKIRSEELSFTAVSNGPKNIS GQSPARTSSDPETNTTNEDHKIMASENSSAMVQVHS | 100 | 96.6 | 96.6 | 53.6 | 39.7 |
| III.1 | 210-220 | SSGYYSTTIRY | 100 | 100 | 100 | 45.4 | 36.3 |
| III.2 | 226-253 | GTNETEYLFEVDNLTYVQLESRFTPQFL | 100 | 100 | 100 | 78.5 | 46.4 |
| III.3 | 258-299 | ETIYASGKRSNTTGKLIWKVNPEIDTTIGEWAFWETKK NLTR | 100 | 97.6 | 97.6 | 73.8 | 54.7 |
| IV | 267-419 | SNTTGKLIWKVNPEIDTTIGEWAFWETKKNLTRKIRSE ELSFTAVSNGPKNISGQSPARTSSDPETNTTNEDHKI MASENSSAMVQVHSQGRKAAVSHLTTLATISTSPQPP TTKTGPDNSTHNTPVYKLDISEATQVGQHHRRADNDS TASD | 100 | 93.4 | 94.7 | 30 | 26.7 |
| IV.1 | 282-305 | DTTIGEWAFWETKKNLTRKIRSEE | 100 | 100 | 100 | 66.6 | 62.5 |
| IV.2 | 286-296 | GEWAFWETKKN | 100 | 100 | 100 | 90.9 | 90.9 |
| IV.3 | 286-364 | GEWAFWETKKNLTRKIRSEELSFTAVSNGPKNISGQS PARTSSDPETNTTNEDHKIMASENSSAMVQVHSQGR KAAVSH | 100 | 94.2 | 94.2 | 37.1 | 35.7 |
| IV.4 | 326-414 | TSSDPETNTTNEDHKIMASENSSAMVQVHSQGRKAA VSHLTTLATISTSPQPPTTKTGPDNSTHNTPVYKLDIS EATQVGQHHRRADND | 100 | 91 | 93.2 | 13.4 | 11.2 |
| V | 336-582 | NEDHKIMASENSSAMVQVHSQGRKAAVSHLTTLATIS TSPQPPTTKTGPDNSTHNTPVYKLDISEATQVGQHHR RADNDSTASDTPPATTAAGPLKAENTNTSKSADSLDL ATTTSPQNYSETAGNNNTHHQDTGEESASSGKLGLIT NTIAGVAGLITGGRRTRREVIVNAQPKCNPNLHYWTT QDEGAAIGLAWIPYFGPAAEGIYTEGLMHNQDGLICGL RQLANETTQALQLFLRATTELRTF | 100 | 93.9 | 95.1 | 42.5 | 35.6 |
| V.1 | 343-368 | ASENSSAMVQVHSQGRKAAVSHLTTL | 100 | 96.1 | 96.1 | 19.2 | 19.2 |
| V.2 | 372-420 | STSPQPPTTKTGPDNSTHNTPVYKLDISEATQVGQHH RRADNDSTASDT | 100 | 89.7 | 93.8 | 10.2 | 12.2 |
| V.3 | 380-491 | TKTGPDNSTHNTPVYKLDISEATQVGQHHRRADNDST ASDTPPATTAAGPLKAENTNTSKSADSLDLATTTSPQ NYSETAGNNNTHHQDTGEESASSGKLGLITNTIAGVA G | 100 | 92 | 92.9 | 15 | 15.9 |
| V.4 | 424-447 | TTAAGPLKAENTNTSKSADSLDLA | 100 | 83.3 | 83.3 | 0 | 4.1 |
| V.5 | 436-491 | NTNTSKSADSLDLATTTSPQNYSETAGNNNTHHQDT GEESASSGKLGLITNTIAGVAG | 100 | 92.8 | 91 | 19.6 | 16 |
| V.6 | 456-484 | SETAGNNNTHHQDTGEESASSGKLGLITN | 100 | 100 | 100 | 17.2 | 20.6 |
| V.7 | 469-498 | TGEESASSGKLGLITNTIAGVAGLITGGRR | 100 | 100 | 100 | 50 | 30 |
| V.8 | 367-378 | TLATISTSPQPP | 100 | 83.3 | 100 | 83 | 0 |
| V.9 | 520-547 | TQDEGAAIGLAWIPYFGPAAEGIYTEGL | 100 | 96.4 | 100 | 96.4 | 71.4 |
| V.10 | 585-599 | LNRKAIDFLLQRWGG | 100 | 100 | 100 | 100 | 93.3 |
| V.11 | 439-465 | KSADSLDLATTTSPQNYSETAGNNNTH | 100 | 85.1 | 81.4 | 3.7 | 3.7 |
| VI | 617-645 | KNITDKIDQIIHDFVDKTLPDQGDNDNWW | 100 | 100 | 100 | 89.6 | 72.4 |
| VII | 603-624 | ILGPDCCIEPHDWTKNITDKID | 100 | 100 | 100 | 100 | 95.4 |

## TRANSPARENT METHODS:

### Proteins, Plasma samples and Monoclonal Antibodies

Recombinant EBOV glycoproteins (GP residues Met1-Gln650 containing the transmembrane domain) used in this study were purchased from Sino Biologicals Inc. The clinical plasma samples were obtained from NIBSC as part of a "WHO collaborative study to assess the suitability of an interim standard for antibodies to Ebola virus" (Supplementary Table 1)(Wilkinson et al., 2017). Briefly, plasma obtained from convalescent patients recovered from Ebola virus disease and were negative for Ebola virus RNA and other blood viral markers [Norway (NOR; #43, 2 months post infection), American Red Cross (ARC; #79, 3 months post infection), and National Health Service Blood and Transplant (NHSBT; #28, 6 months post infection)]. A pooled convalescent plasma (sample #92) was obtained from six Sierra Leone patients recovered from EVD who did not receive any Ebola-specific treatment (Supplementary Table 1). These patients did not receive any Ebola-specific treatment. The PCR-negative plasmas were solvent-detergent-extracted using a method validated at NIBSC. The Norwegian patient received ZMapp (anti-GP), Favipiravin (RNA pol inhibitor) and TKM-10000802 (iRNA). The NHSBT patient received Brincidifovar (antiviral) and convalescent plasma treatments. The ARC patient received convalescent plasma as well as infusions of TKM-Ebola (iRNA). WHO study established sample #79 as the WHO International Reference Reagent (NIBSC product code 15/220) with an assigned potency of 1 unit/mL. This is equivalent to 0.68 International Units/mL (95% CI 0.57-0.80) when calibrated against the 1st International Standard for Ebola Antibody (NIBSC code 15/262) (http://www.who.int/biologicals/expert_committee/BS2316_Anti-EBOV_Antibodies_WHO_1st_IS_and_WHO_1st_International_Ref_Panel.pdf).

Pooled vaccinee plasma were obtained from volunteers participating in Oxford, UK vaccine trial(Ewer et al., 2016) . The protocol consisted of priming with chimpanzee adenovirus 3 (ChAd3)–vectored vaccine encoding the surface glycoprotein of EBOV/Mayinga and boosting with the same EBOV GP gene in a modified vaccinia Ankara (MVA)-vectored vaccine that also contains SUDV and MARV (Marburg virus) glycoproteins, and TAFV (Tai Forest ebolavirus) nucleoprotein(Wilkinson et al., 2017). Since there were only small volumes from several individual vaccinees, pools with low (Sample #64) or high (Sample #58) neutralization titers were generated from individual samples with "low" or "high" neutralization titers obtained and used as a part of the WHO collaborative study(Wilkinson et al., 2017). The ChAd3-MVA prime-boost post-vaccination samples were a mix of different time points (2 - 12 months) post-vaccination following booster vaccination. Samples were anonymous, and permission to test these de-identified samples in different antibody assays was obtained from the U.S. Food and Drug Administration's Research Involving Human Subjects Committee (FDA-RIHSC) under exemption protocol #15-0B.

### Binding of human plasma to recombinant GP, isotyping and off-rate measurements by Surface Plasmon Resonance (SPR)

Steady-state equilibrium binding of post-EBOV infected survivor and post-vaccinated human polyclonal plasma was monitored at 25°C using a ProteOn surface plasmon resonance (Bio Rad). The purified recombinant GP (GP residues Met1-Gln650 containing the transmembrane domain) were coupled to a GLC sensor chip via amine coupling with either 100 or 500 resonance units (RU) in the test flow channels. The protein density on the chip was optimized such as to measure only monovalent interactions independent of the antibody isotype. Serial dilutions of freshly prepared plasma in BSA-PBST buffer (PBS pH 7.4 buffer with Tween-20 and BSA) were injected at a flow rate of 50 µl/min (120 sec contact duration) for association, and disassociation was performed over a 1200-second interval. Responses from the protein surface were corrected for the response from a mock surface and for responses from a buffer-only injection. SPR was performed with serially diluted plasma of each individual sample in this study. Sensorgram for a representative sample dilution is shown in Supplementary figure 1.

Antibody isotype analysis for the GP bound antibodies in the polyclonal plasma was performed using SPR. Secondary MAb analytes with similar affinity/binding patterns with specificity against Fc region of either human IgG1, IgG2, IgG3, IgG4, IgA or IgM were used for istyping. Total antibody binding and antibody isotype analysis were calculated with BioRad ProteOn manager software (version 3.1). All SPR experiments were performed twice and the researchers performing the assay were blinded to sample identity. In these optimized SPR conditions, the variation for each sample in duplicate SPR runs was <5%.

Antibody off-rate constants, which describe the stability of the antigen-antibody complex, i.e. the fraction of complexes that decays per second, were determined directly from the human polyclonal plasma sample interaction with rGP protein using SPR (as described above) and calculated using the BioRad ProteOn manager software for the heterogeneous sample model.

**Gene Fragment Phage Display Library (GFPDL) construction**

cDNA complementary to the envelope glycoprotein gene of Ebola virus Makona strain was chemically synthesized and used for cloning. A gIII display-based phage vector, fSK- 9-3, was used where the desired polypeptide can be displayed on the surface of the phage as a gIII-fusion protein. Purified DNA containing EBOV *GP* was digested with *DNase I* to obtain gene fragments of 50-1000 bp size range and used for GFPDL construction as described previously(Khurana et al., 2016). Since the phage libraries were constructed from the whole Ebola surface glycoprotein gene, they potentially display all possible known or unknown viral protein segments ranging in size from 15 to 350 amino acids, as fusion protein on the surface of bacteriophage (Supplementary figure 3).

**Adsorption of polyclonal human survivor plasma on EBOV GFPDL phages and residual reactivity to Makona-GP**

Prior to panning of GFPDL, 500 μl of 10-fold diluted serum antibodies from post-infection survivor plasma sample #79 was adsorbed by incubation with EBOV GFPDL phage-coated Petri dishes. To ascertain the residual antibodies specificity, an ELISA was performed with wells coated with 200 ng/100 μl of recombinant Makona-GP. After blocking with PBST containing 2% milk, serial dilutions of human plasma (with or without adsorption) in blocking solution were added to each well, incubated for 1 hr at RT, followed by addition of 5000-fold diluted HRP-conjugated goat anti-human IgA + IgG + IgM specific antibody and developed by 100 μl of OPD substrate solution. Absorbance was measured at 490 nm.

**Affinity selection of EBOV-GP GFPDL phages with polyclonal human plasma**

Prior to panning of GFPDL with polyclonal plasma antibodies, plasma components that could non-specifically interact with phage proteins were removed by incubation with UV-killed M13K07 phage-coated Petri dishes. Equal volumes of each human plasma were used for GFPDL panning. GFPDL affinity selection was carried out in-solution (with Protein A/G) as previously described (Khurana et al., 2009; Khurana et al., 2011). The GFPDL affinity selection data was performed in duplicate (independent experiments by two different research fellows in the lab, who were blinded to sample identity), and similar number of phage clones and epitope repertoire observed in all four-phage display library analysis. A model for the complete Zaire strain GP was generated using I-TASSER(Yang et al., 2015) and was used to represent the antigenic sites on the structure. Crystal structure of EBOV GP (PDB Id #3CSY; for EBOV/Mayinga or the PDB Id #6DZL for EBOV/Makona) was used as a reference (Lee et al., 2008).

**Statistical Analyses**

The statistical significances of group differences were determined using an Ordinary one-way ANOVA and Tukey's multiple comparisons method. *p*-values less than 0.05 were considered significant with a 95% confidence interval. Correlations were calculated with a Pearson method and P value for correlation was calculated by two-tailed test.

## SUPPLEMENTAL REFERENCES

Ewer, K., Rampling, T., Venkatraman, N., Bowyer, G., Wright, D., Lambe, T., Imoukhuede, E.B., Payne, R., Fehling, S.K., Strecker, T.*, et al.* (2016). A Monovalent Chimpanzee Adenovirus Ebola Vaccine Boosted with MVA. N Engl J Med *374*, 1635-1646.

Khurana, S., Fuentes, S., Coyle, E.M., Ravichandran, S., Davey, R.T., Jr., and Beigel, J.H. (2016). Human antibody repertoire after VSV-Ebola vaccination identifies novel targets and virus-neutralizing IgM antibodies. Nat Med *22*, 1439-1447.

Khurana, S., Suguitan, A.L., Jr., Rivera, Y., Simmons, C.P., Lanzavecchia, A., Sallusto, F., Manischewitz, J., King, L.R., Subbarao, K., and Golding, H. (2009). Antigenic fingerprinting of H5N1 avian influenza using convalescent sera and monoclonal antibodies reveals potential vaccine and diagnostic targets. PLoS Med *6*, e1000049.

Khurana, S., Verma, N., Yewdell, J.W., Hilbert, A.K., Castellino, F., Lattanzi, M., Del Giudice, G., Rappuoli, R., and Golding, H. (2011). MF59 adjuvant enhances diversity and affinity of antibody-mediated immune response to pandemic influenza vaccines. Sci Transl Med *3*, 85ra48.

Lee, J.E., Fusco, M.L., Hessell, A.J., Oswald, W.B., Burton, D.R., and Saphire, E.O. (2008). Structure of the Ebola virus glycoprotein bound to an antibody from a human survivor. Nature *454*, 177-182.

Wilkinson, D.E., Page, M., Mattiuzzo, G., Hassall, M., Dougall, T., Rigsby, P., Stone, L., and Minor, P. (2017). Comparison of platform technologies for assaying antibody to Ebola virus. Vaccine *35*, 1347-1352.

Yang, J., Yan, R., Roy, A., Xu, D., Poisson, J., and Zhang, Y. (2015). The I-TASSER Suite: protein structure and function prediction. Nat Methods *12*, 7-8.